Self-Healing Photochromic Elastomer Composites for Wearable UV-Sensors

Tiwa Yimyai, Daniel Crespy,* and Abdon Pena-Francesch*

Photochromic materials have recently received strong interest for the development of wearable ultraviolet (UV) detection technologies because they do not require electronic components, resulting in systems and devices that change color upon irradiation. However, their implementation in wearable technology has lightweight, compliance, and durability (especially under mechanical stress) requirements that are limited by the materials' properties. Here, a self-healing photochromic elastomer composite (photoPUSH) consisting of phosphomolybdic acid (PMA) in a self-healing polyurethane dynamic network with reversible disulfide bonds (PUSH) is presented. The unique properties of the dynamic polymer matrix enable multiple complementary functions in the UV-sensing composite: i) photochromism via electron donor groups without requiring additional dopants, ii) stretchability and durability via elastomeric properties, iii) healing of extreme mechanical damage via dynamic bonds, and iv) multimaterial integration via adhesive properties. PhotoPUSH composites exhibit excellent durability, tunable sensing range, and no loss of performance under mechanical stress and severe damage, as well as in underwater environments (waterproof). Leveraging these properties, soft, portable, multimaterial photoPUSH-based UV-sensing devices are developed for applications in environmental monitoring, packaging, and healthcare wearable technology (including skin-mounted, textile-mounted, and wristband devices) in challenging environments and tunable to different skin types.

1. Introduction

Ultraviolet (UV) light is a type of electromagnetic radiation that can be generated naturally or synthetically and can be either potentially beneficial or harmful. Synthetic UV light is abundantly utilized in the healthcare industry (in the disinfection of medical surfaces and devices, or in the production of vitamin D, and in phototherapy and photoimaging)[1–4] as well as in industrial manufacturing processes such as 3D printing, photocuring of polymers, and laser micromachining. However, overexposure to UV light can be harmful to human health, including eye damage, skin damage, and immune system suppression.[5] In particular, the UV light penetrating into the skin can be absorbed by cellular chromophores (e.g., hemoglobin, melanin, DNA, and nucleic acids), resulting in the production of free radicals or reactive oxygen species.[6] The generated reactive species cause oxidation of biological macromolecules (proteins, lipids, and nucleic acids) and cellular components in the skin, which leads to skin inflammation, skin aging, and ultimately skin cancer.[7–9] It was estimated that more than 419,000 cases of UV-induced skin cancer (basal cell carcinomas, squamous cell carcinomas, or melanomas) occur each year in the United States,[10] with an annual cost of direct medical care of ≈343 million dollars.[11] Therefore, monitoring of UV light exposure is essential to ensure safe protection and to avoid UV-derived health problems. Most commercial UV sensors are mainly in the form of electronic solid-state devices,[12–14] which are typically rigid and fragile, limiting their portability and their application in the field due to a lack of compliance and resiliency.

In recent years, wearable UV sensors have been developed to monitor exposure for healthcare applications, with major advantages in portability enabling easy point-of-care testing and real-time monitoring in the field.[15–17] Current wearable UV sensing technologies can be categorized into photoelectric and photochromic systems.[15] Photoelectric sensors are typically composed of photodetectors,[18–21] which rely on sensing through conversion of UV irradiation to electric current via photoexcitation of electrons in bandgap of semiconductor materials. For example, photodetectors have integrated metal oxides[22] (such as zinc oxide, titanium dioxide, tin (IV) oxide, and vanadium pentoxide) or multielement alloys[21,23] (such as indium gallium nitride and aluminum gallium nitride) to

T. Yimyai
Department of Chemical and Bimolecular Engineering
School of Energy Science and Engineering
Vidyasirimedhi Institute of Science and Technology (VISTEC)
Rayong 21210, Thailand

T. Yimyai, D. Crespy
Department of Materials Science and Engineering
School of Molecular Science and Engineering
Vidyasirimedhi Institute of Science and Technology (VISTEC)
Rayong 21210, Thailand
E-mail: daniel.crespy@vistec.ac.th

T. Yimyai, A. Pena-Francesch
Department of Materials Science and Engineering, Macromolecular
Science and Engineering, Robotics Institute
University of Michigan
Ann Arbor, Michigan 48109, USA
E-mail: abdon@umich.edu

The ORCID identification number(s) for the author(s) of this article can be found under https://doi.org/10.1002/adfm.202213717.

**ADVANCED
SCIENCE NEWS**

www.advancedsciencenews.com

**ADVANCED
FUNCTIONAL
MATERIALS**

www.afm-journal.de

adjust their bandgap energy or charge carrier transport channels, resulting in enhanced wavelength selectivity or photoresponse, respectively. Nevertheless, photoelectric sensors must transform photocurrent into measurable electronic signals,[15,22] and therefore require additional electronic components (such as spectroradiometers) that complicate their miniaturization and their integration into wearable devices. Furthermore, these additional components make the sensors rigid, fragile, and with limited application in wearable technology.

On the other hand, photochromic sensors do not require additional electronic components for a direct visual colorimetric measurement and they can be integrated into soft, flexible, and conformable materials, which makes them more attractive for the development of soft wearable sensors and devices.[15,24–26] Photochromic sensors undergo a color change upon UV light exposure due to photoreactions of functional groups in their molecular structures or charge transfer in redox reactions.[24,27] For example, color change of organic photochromic dyes has been previously achieved via photocyclizations of spiropyran[28] and diarylethene[29] derivatives upon UV irradiation. Photoinduced color change of soft UV sensors has been also achieved by cleaving *ortho*-nitrobenzyl moieties to form azo groups,[30] and by *trans–cis* isomerization of azobenzene molecules[31] under UV light. Color-switching of tungsten-,[32,33] molybdenum-,[34] and titanium-[35] based photochromic composites was also generated upon UV exposure by reduction reactions of the transition metals, resulting in a change of their valence state, and consequently forming mixed-valence colored species.

Polyoxometalates (POMs) have been recently introduced as photochromic materials for UV sensors[36–38] owing to their fast multi-electron transfer reactions upon UV irradiation, long-term photochemical stability, and good sensitive coloration.[39] The charge transfer reactions between POMs and electron donors induce a reduction of the central metals in POMs, resulting in a deep-blue color for UV-sensing function.[40] Because of this mechanism, POM-based sensors require additional chemicals as electron donor groups to activate the color change in the system, which can be incorporated either as additives (lactic or citric acids) in paper-based sensors[36,41] or as polymer matrices in composite systems (such as poly(acrylic acid),[33] polyvinylpyrrolidone,[42,43] polyacrylamide,[44] poly(ethylene glycol),[45] and cellulose[37]). However, although flexible, the resulting POM-based sensors exhibit low durability due to the low mechanical strength and stability of these polymer matrices and fillers and are therefore vulnerable to mechanical damage, scratches, and exposure to environmental factors (such as water) that deteriorate their performance.

To address these durability and vulnerability challenges, self-healing soft materials present unique opportunities to enable resilient UV-sensing devices that can reliably perform in realistic environments. Self-healing soft materials relying in dynamic covalent bonds and reversible crosslinking mechanisms have been extensively studied in recent years,[46] and have been implemented in soft devices in an array of applications ranging from information storage[47] to sensing[48,49] to robotics.[50,51] However, many self-healing polymers present fundamental materials challenges to perform effectively in wearable photochromic applications, for example, they should have high healing efficiency to recover their properties without

loss of function, resist common chemical hazards relevant to their use (insensitive to water and other environmental factors), and they must be optically transparent to enable photochromic sensing. Self-healing polymers composed of dynamic disulfide bonds are of special interest here since they exhibit excellent healing efficiency (> 95%) at moderate temperatures (25–80 °C) due to a low bond dissociation energy, and they can be introduced into polyurethane polymers to confer healing properties to the network while retaining optical transparency.[52]

Here, we develop a new type of multifunctional photochromic elastomer composite with self-healing and UV-responsive properties by incorporating phosphomolybdic acid (PMA) into a self-healing polyurethane (PUSH) polymer network with dynamic disulfide bonds. The integration of PMA in PUSH polymers results in synergistic properties and capabilities that are not achieved with other material combinations: i) provides electron donor functional groups to enable the photochromic mechanism and the UV-sensing, thus eliminating the need for electron donor additives, ii) enables the fabrication of composites by directly dispersing the active photochromic dopant into a mechanically stable and protective matrix, eliminating the dependence on other substrates, iii) provides healing properties to the nanocomposite, with high healing efficiency and recovery of functions after extreme mechanical damage, iv) provides adhesive properties to a variety of surfaces to enable the use as smart photochromic sticker sensors, and v) enables the interfacial bonding of PUSH-based materials with different compositions, allowing for the fabrication of stretchable multimaterial devices without delamination or fracture limitations. The self-healing photochromic polyurethane elastomers composites (photoPUSH) exhibited programmable sensitivity to UV light, displaying a visual color change through photoreduction of PMA molecules without adding additives, as well as excellent durability to mechanical stress, water-resistance, and healing efficiency (> 97%). By tailoring their composition, photoPUSH soft composites were designed with a programmable photochromic response for a broad range of UV doses, thus providing a sensing platform for the safe UV exposure threshold for different skin types. We demonstrate the application of the photoPUSH composites as adhesive sensor stickers for environmental monitoring and for skin-mounted, textile-integrated, and bracelet-type wearable sensors.

2. Results and Discussion

2.1. Photochromic Properties

Phosphomolybdic acid (PMA) was incorporated as a UV-sensing nanofiller by taking advantage of its photochromic properties and resulting color change upon exposure to UV light. The color change of PMA can be activated with electron-donating groups such as amine[42,44] and alcohol[37,45,53] groups in molecular structures of complementary polymers under UV light exposure. Consequently, molybdenum (Mo) metals in the Keggin structure of PMA were reduced from Mo^{6+} to Mo^{5+} and converted into heteropolyblues via multi-electron transfer reactions in a photochemical reduction process.[54,55] In this work, we incorporated PMA in a self-healing polyurethane

ADVANCED
SCIENCE NEWS
www.advancedsciencenews.com

ADVANCED
FUNCTIONAL
MATERIALS
www.afm-journal.de

matrix (PUSH), which was synthesized by addition polymerization of polytetrahydrofuran (PTHF), dicyclohexylmethane 4,4'-diisocyanate (HMDI) and 2-hydroxyethyl disulfide (HEDS) (Figure S1, Supporting Information). The photochromic reaction between PMA and PUSH with increasing UV exposure was monitored by FTIR spectroscopy. FTIR spectra displayed characteristic bands of PMA at 1060, 963, 881, and 777 cm^{-1} for P—O$_a$ stretching, Mo=O$_d$ stretching, Mo—O$_b$—Mo stretching, and Mo—O$_c$—Mo stretching, respectively and characteristic bands of PUSH at 1229–1247 and 1110 cm^{-1} for C—N stretching and C—O—C stretching, respectively (Figure S2, Supporting Information). In photoPUSH films, the characteristic bands of PMA were shifted to 1065, 960, 880, and 812 cm^{-1} for P—O$_a$ stretching, Mo=O$_d$ stretching, Mo—O$_b$—Mo stretching, and Mo—O$_c$—Mo stretching, respectively, signaling the intermolecular forces between Keggin structures of PMA and the PUSH polymer matrix (**Figure 1**a; Figure S2, Supporting information). Upon UVA light irradiation, the characteristic bands of PMA in the photoPUSH showed a red shift and their intensity decreased owing to the reduction of PMA after accepting protons from the PUSH matrix to form heteropolyblues. The decreased intensity of the FTIR bands associated to heteropolyblues is in agreement with other reports of the same photochromic mechanism in the literature (with hydroxyl and amino groups as donors).[37,45,53,56,57] However, while previous reports of PMA-photochromic sensor materials relied on PMA/polymer systems or ink solutions with electron donor additives that were deposited on rigid and non-stretchable substrates,[33,36,37,41–45] photoPUSH composites incorporate electron donor groups directly into the polyurethane elastomer structure, resulting in a stretchable, monolithic, photochromic material. In this approach, PUSH polymers to provide structural and photochromic functions simultaneously, thus eliminating the need for organic electron donor additives or rigid substrates that are required in previous approaches. To highlight the important role of the polymer matrix in the photochromic mechanism and to evaluate the synergistic properties of the PUSH materials developed here, we benchmarked different common substrates and flexible polymer materials by depositing a layer of PMA and observing the color change with UV exposure (Figure S3, Supporting Information). While most substrates did not exhibit any color change due to the lack of electron donor groups, PMA deposited on PUSH and PUHD (control polyurethane elastomer without disulfide bonds) substrates exhibited a sharp shift from colorless to blue (Figure 1b; Figure S3, Supporting Information), which became more intense with an increasing amount of PMA and increasing exposure time. These results indicated that PUSH polymers
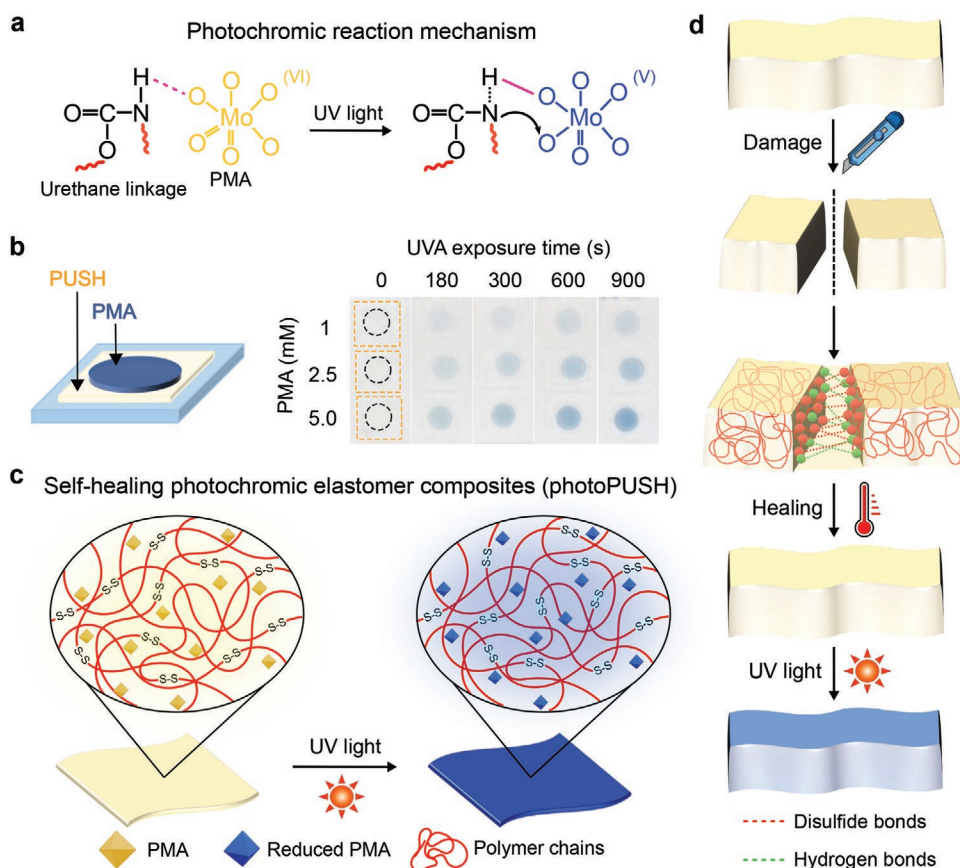

Figure 1. a) Photochromic mechanism between phosphomolybdic acid hydrate (PMA) and urethane groups in a self-healing polyurethane (PUSH) polymer network. b) PMA deposited on a PUSH polymer film, showing color change after exposure to UVA light. c) Photochromic elastomer composites (photoPUSH) with a color change after exposure to UV light. d) The photoPUSH composite is capable of self-healing after damages upon activation with temperature, and still displays color change upon UV light exposure.

can act as an electron donor active matrix (due to its urethane groups) (Figure 1c), thus eliminating the need for additives and external electron donors typically required in other UV-sensing formulations (such as citric acid[41] or lactic acid[36]). Therefore, in addition to their mechanical, healing, and adhesive properties (described in detail afterward), the PUSH polymers developed in this work directly enable the photochromic properties in PMA composites, therefore performing multiple functions simultaneously in this materials system (Figure 1d).

In order to characterize the response to UV light, we measured the color change of photoPUSH films upon exposure to UVA (λ_{max} = 368 nm), UVB (λ_{max} = 306 nm), and UVC (λ_{max} = 265 nm) radiation. As shown in **Figure 2**a, the absorption intensity at a wavelength of 760 nm of photoPUSH films increased with UVA, B, and C doses until it reached a plateau. The increase of absorption intensity at a wavelength of ≈760 nm reflects the visible color change of photoPUSH with UV irradiation (Figure 2b), which corresponds to the reduction of Mo^{6+} to Mo^{5+} in the Keggin structure of PMA.[54] PhotoPUSH films displayed the largest responsivity to UVA, followed by UVB, and UVC according to the highest absorbance at a plateau. This is largely caused by different absorption of UVA, B, and C light by the PUSH matrix, (Figure S4, Supporting Information). Therefore, photoPUSH exhibited spectral selectivity (differentiation of absorbance among UVA, B, and C) when exposed to the different UV light doses with more than 50 kJ m^{-2}. It is generally accepted that UVB has high risk of inducing skin cancer due to its involvement in the direct photochemical damage to DNA.[58,59] However, UVA light was targeted for sensing in this

work due to the fact that 95% of UV rays reaching the earth's surface are UVA rays. In addition, UVA rays penetrate deeper into the skin and are absorbed by endogenous photosensitizers in human skin to generate radicals or reactive oxygen species, which can damage DNA and increase the risk of melanoma and other types of skin cancer.[59–61] Therefore, UVA is considered a better indicator of UV dose, which can in turn be used to calculate UVB and UVC. PhotoPUSH composites with different amounts of PMA were illuminated with different doses of UVA light (λ_{max} = 368 nm) and characterized (Figure 2c). After UVA irradiation, the color of photoPUSH films with 0.1 and 0.2 wt.% PMA did not significantly change and was similar to the control PUSH film. PhotoPUSH films with 1.1, 1.8, 2.3, and 5.7 wt.% PMA displayed a color change from colorless to blue, and the films with 11.4, 22.8, and 34.2 wt.% PMA turned from yellow to dark green and to dark blue with increasing UVA dose. The photochromic effect was measured in the 0 to 40 °C temperature range (Figure S5, Supporting Information), without significant changes in color change with UVA dose or saturation color (indicating that this materials system is stable and not affected by temperature fluctuations within this range). In addition, the dark saturated colors are highly stable and are preserved for at least 22 days without any exposure to UV light (dark conditions) (Figure S6, Supporting Information). However, if desired, the color change in the material can be reversed chemically by inducing the oxidation of the PMA molecules (Figure S7, Supporting Information).[62] This reversible color change can enable the use of the composite materials over multiple cycles.
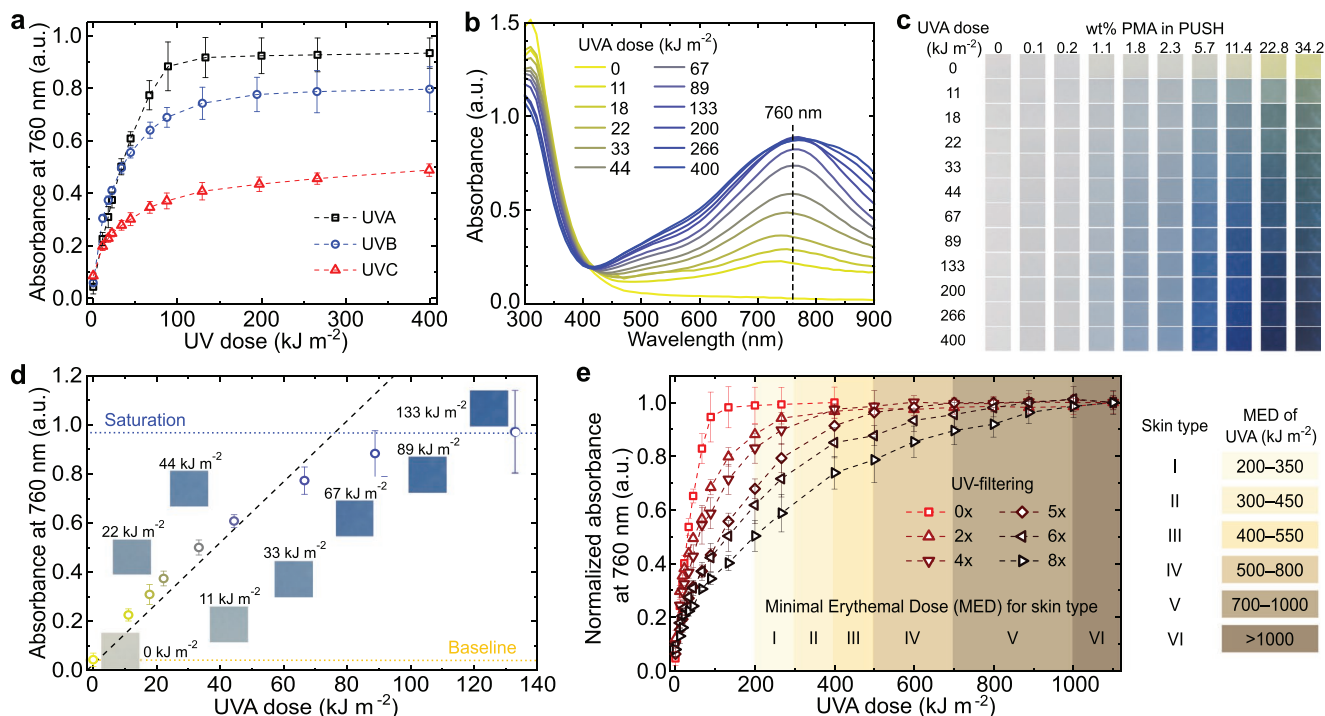

Figure 2. a) Absorbance at 760 nm as a function of UVA, B, and C light doses in photoPUSH films with 5.7 wt.% PMA. b) UV–vis absorbance spectra of a photoPUSH (5.7 wt.% PMA) with increasing exposure to UVA light. c) Color change of photoPUSH with different amounts of PMA with increasing doses of UVA light. d) Absorbance at 760 nm as a function of UVA light dose for a photoPUSH film (5.7 wt.% PMA). e) Normalized absorbance at 760 nm as a function of UVA light dose for photoPUSH (5.7 wt.% PMA) films with integrated filtering tailored to match the MED for skin types I through VI.

ADVANCED
SCIENCE NEWS
www.advancedsciencenews.com

ADVANCED
FUNCTIONAL
MATERIALS
www.afm-journal.de

The absorbance at 760 nm was used to quantify the reduction of PMA at a certain dose of UVA light exposure (Figure S8, Supporting Information) and to quantitatively monitor the photochromic evolution with UVA light in the full range of PMA amounts in PUSH. The absorption saturation was reached when most of the PMA molecules were reduced to heteropolyblues, which varied with amount of PMA. A photoPUSH with 5.7 wt.% PMA was selected as the model formulation for photoPUSH photochromic composites due to its gradual change from colorless to blue with an initial linear increase of absorbance at 760 nm with UVA dose (Figure 2d). The absorption intensity reached a plateau at a UVA dose of 130 kJ m^{-2}, resulting in a saturated blue color that remained constant upon further irradiation. This saturation dose delimitates the UV sensing range of the composites; however, UV radiation affects each skin type differently (melanin, present at different concentrations in different skin types, is a UV absorber that reduces the penetration of UV through epidermis).[63] Therefore, to expand the sensing range of photoPUSH composites, the saturation threshold dose was increased by integrating melanin-mimicking thin film UV filters (Figure S9, Supporting Information).[36] As shown in Figure 2e, the absorbance at 760 nm (i.e., color change) of photoPUSH composites with integrated filters increases more slowly with UVA dose, and the saturation threshold is delayed and extended to larger UVA doses (higher exposure). Therefore, with careful materials design, photoPUSH composites with integrated filtering can be used as film sensors to track UVA radiation with a visible color change within a tunable dose range and threshold that can be adjusted to different skin types. The capacity of each skin type to resist sunburn is determined by the lowest UV dose called minimal erythemal dose (MED).[64] Hence, photoPUSH composite films with UV filtering of 0x, 2x, 4x, 5x, 6x, and 8x were fabricated for UVA detection of skin types I through VI, respectively (Figure 2e). The saturation threshold of each sensor was adjusted to match the MED for different skin types, so the sensor saturates in a dark blue color when entering a specific MED (potentially hazardous dose) and alerts the user to avoid further exposure.

2.2. Mechanical and Healing Properties of PhotoPUSH

In order to evaluate photoPUSH composite elastomers as potential wearable sensors, their stability and durability under mechanical stress were characterized. First, we explored three different fabrication methods to incorporate PMA dopants into the self-healing materials: i) directly depositing PMA ink on a PUSH substrate (previously used in PMA photochromic devices),[36,38,41,62] ii) depositing a PMA ink layer and encapsulating it between two PUSH layers, and iii) dispersing PMA in the bulk PUSH matrix (photoPUSH). Although PMA was homogeneously dispersed, i) and ii) showed cracking when stretched (**Figure 3**a). The ink-deposited PMA layer i) showed cracking perpendicular to the strain throughout all the deposited areas. The encapsulated layer ii) exhibited similar cracking, but only on the edges. However, PMA dispersed in the bulk (hereinafter referred to as photoPUSH) exhibited good mechanical stability and strong interfacial bonding between PMA and the PUSH matrix, and did not exhibit any visible signs of cracking, delamination, or any noticeable defect (under ≈100% strain). The mechanical properties of photoPUSH (5.7 wt.% PMA) were further evaluated through tensile testing with dog-bone tensile specimens. The average tensile strength (σ) of pristine PUHD (control polyurethane without disulfide
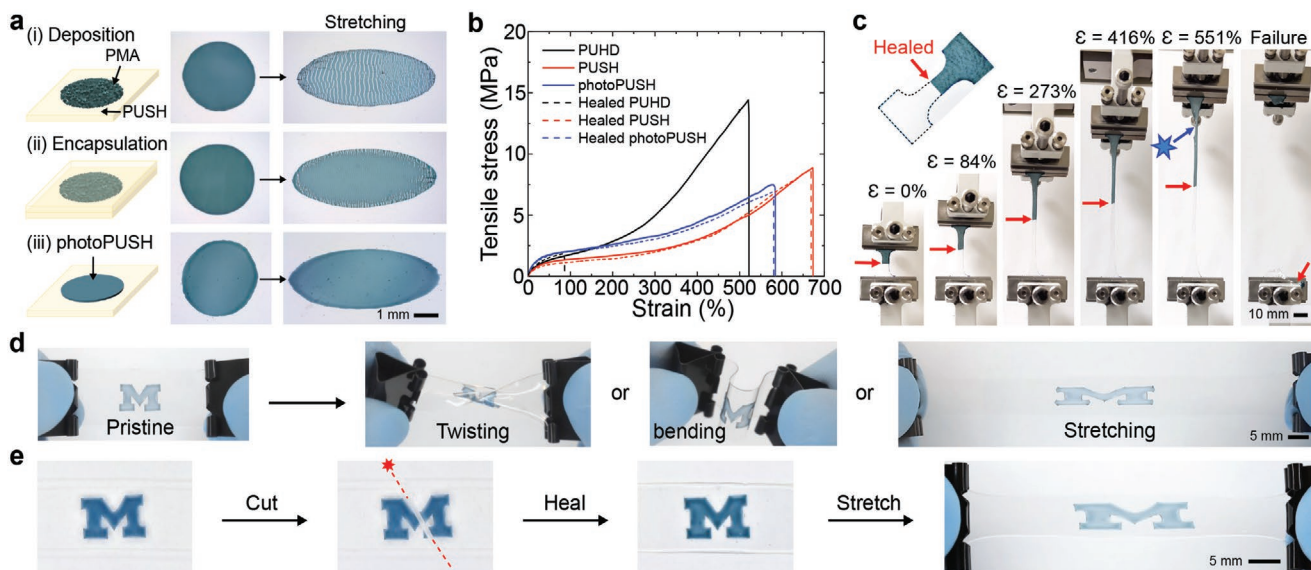

Figure 3. a) Stability under 100% strain of i) PMA deposited on a PUSH substrate, ii) a PMA layer encapsulated between two PUSH layers, and iii) a homogeneous photoPUSH film. b) Tensile stress–strain curves of pristine and healed PUHD, pristine and healed PUSH films, pristine and healed photoPUSH with 5.7 wt.% PMA. The polymer films were healed at 70 °C for 24 h. c) A dog-bone specimen composed of healed PUSH (transparent) and photoPUSH (blue) was stretched to failure and fractured at random pristine locations. d) A "M"-shaped photoPUSH film was bonded to a PUSH film by healing at 70 °C for 24 h. The "M" photoPUSH film was manipulated by twisting, bending, and stretching with an elongation of 140%, showing no visible damage or delamination. e) "M" photoPUSH was cut into separate pieces and was subsequently healed at 70 °C for 24 h. The healed photoPUSH was stretched to 150% strain with no visible damage or delamination.

bonds), PUSH (control without PMA), and photoPUSH was 14.6 ± 1.2, 8.1 ± 0.8, and 7.4 ± 0.5 MPa respectively, while average ultimate strain (ε) of pristine PUHD, PUSH, and photoPUSH was 496 ± 31, 613 ± 55, and 544 ± 41%, respectively (Figure 3b). We also measured the effect of UV light on the creep of PUSH elastomers under shear with a constant stress of 0.1 MPa (Figure S10, Supporting Information), without observing any significant difference in creep behavior.

To investigate the healing ability of the composites, dog-bone tensile specimens were cut into two pieces and joined together at the cut, followed by healing at 70 °C for 24 h (Figure S11, Supporting Information). σ and ε of healed PUHD were 1.9 ± 0.2 and 92 ± 15%, which were much lower than pristine PUHD, whereas the σ and ε of healed PUSH and healed photoPUSH were identical to those pristine samples (Movie S1, Supporting Information). As a result, healing efficiency (the ratio of tensile strength of healed samples to pristine samples) of PUHD, PUSH, and photoPUSH was 13%, 99%, and 97%, respectively. These results indicated that PMA dispersed in PUSH did not affect significantly the self-healing properties. In addition, a healed specimen from PUSH and photoPUSH was stretched until failure, which occurred at a pristine location (Figure 3c), suggesting that the healing efficiency of the photoPUSH was comparable to bare PUSH polymer. The photoPUSH also exhibited good stability and durability under different types of mechanical stress, including twisting, bending, and stretching (Figure 3d; Movie S2, Supporting Information) without any visible damage or delamination, as well as excellent healability after extreme damages such as cutting and scratching of the films (Figure 3e; Figure S12, Supporting Information). These results suggest that both undoped and PMA-doped PUSH elastomers can be joined together and healed with good interfacial strength, thus enabling the integration of photoPUSH in multi-material device designs.

2.3. PhotoPUSH Composites as UV-Sensor Stickers

After understanding and characterizing the photochromic, mechanical, and healing properties, we aimed to develop photo-PUSH-based UV sensors that could be portable and easily implemented on a variety of surfaces. Hence, we fabricated PUSH sensor stickers that adhere to a variety of surfaces taking advantage of the polymer network viscoelasticity. First, we characterized the adhesive properties of PUSH films by measuring the pull-of forces in controlled contact measurements (preload, contact time, loading, and retraction rates) on flat surfaces (**Figure** 4a). The measurements were performed at a minimum of 3 repetitions (adhesion-detachment cycles) per sample and per substrate to confirm that the adhesion is reversible and that the surfaces are not damaged in the process and the adhesion is progressively lost (Figure 4b). We measured the adhesion of PUSH polymer films in a variety of common household substrates (Figure 4c), including polystyrene (63 ± 2 kPa), glass (58 ± 3 kPa), polyethylene (55 ± 1 kPa), PET (35 ± 0.3 kPa), stainless steel (31 ± 0.5 kPa), PUSH (22 ± 1 kPa), paper (22 ± 1 kPa), PDMS (8 ± 0.1 kPa), sandpaper (5 ± 0.1 kPa), and cotton fabric (1 ± 0.1 kPa). These measurements were all performed at room temperature and low preloads (2 N) to simulate gentle pressure

(equivalent to a 0.2 kg force approximately) to adhere to the substrates easily. We observed that the adhesion to rough surfaces was low (e.g., sandpaper, paper, or cotton), however, this can be further improved with higher preloads and higher temperature to increase surface contact.

To take advantage of the adhesion of PUSH to these different substrates and the good healing interfacial bonding strength between PUSH films, UV-sensor stickers were fabricated from a) a bottom PUSH film as an adhesive layer and b) a top patterned photoPUSH film for photochromic display. For example, a photoPUSH UV-sensor sticker (with a photochromic "sun") was attached to a glass window and changed from colorless to blue after being exposed to natural sunlight for 8 h (Figure 4d; Figure S13, Supporting Information). A photoPUSH UV-sensor sticker (with a photochromic warning sign) was attached to the inside of a cardboard storage box (Figure 4e). The colorless appearance of the photoPUSH sticker was stable in the dark (box closed) for over 24 h. When the box was opened and its interior were exposed to ambient light, the sticker gradually shifted to blue color. These proof-of-concept demonstrations highlight the potential of photoPUSH adhesive composites as UV-sensing stickers in various applications, such as monitoring light in photosensitive workspace environments (e.g., cleanrooms and chemical synthesis spaces) or as packaging indicators for shipment, storage, and anti-tampering indicators of photosensitive materials.

2.4. PhotoPUSH for UV-Sensing Wearable Devices

Taking advantage of their elastomeric, healing, and adhesive properties, PUSH-based photochromic composites can be also applied in wearable sensing technology, where continuous use under extreme mechanical stresses and dynamic environments can lead to loss of function and sensing performance. Here, photoPUSH composites with tuned composition were integrated into UV detection patches, which were then mounted on human skin and textiles, as well as in UV detection wristbands. The UV detection patches were fabricated from three layers: (bottom) an adhesive layer for promoting adhesion to skin, (middle) a PUSH layer as a binder to provide bonding strength between all PUSH components, and (top) a UV-sensing layer with a UV detector and colorimetric references (**Figure 5**a). The UV-sensing layer was composed of three control photoPUSH films with 1.1, 1.8, and 5.7 wt.% PMA (low, medium, and high intensities). These reference films were previously exposed to UVA until saturation (constant blue color with different intensities for each composition), therefore providing exterior colorimetric reference to compare with the UV detector. The UV detector consisted of a photoPUSH film with 5.7 wt.% PMA (matching the high-intensity control film), not previously exposed to UV and therefore responsive to light, which will be used to monitor UV exposure. Once assembled, all the components were healed and bonded together yielding a monolithic multimaterial composite film. As shown in Figure 5b, the color of the UV detection patch mounted on the skin gradually evolved toward a dark blue upon cumulative UV irradiation, which can be progressively tracked by comparison with the reference saturated exterior bands. Due to the good
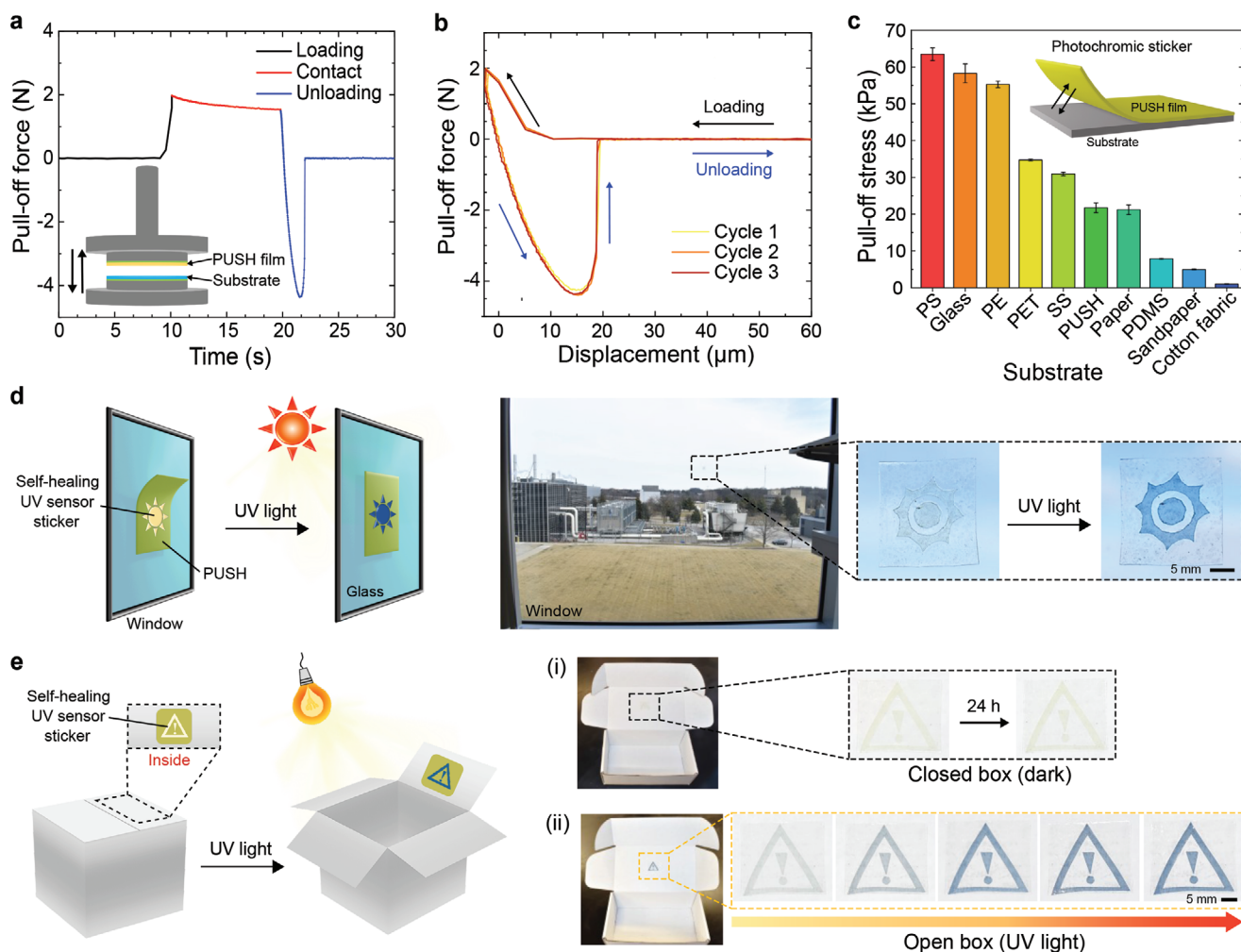
Figure 4. UV-sensor stickers. a) Adhesion pull-off measurements of PUSH films as a function of contact time. b) Reversible adhesion of PUSH over several adhesion cycles. c) Adhesion of PUSH to a variety of common household substrates. d) UV-sensing sticker composed of a patterned photochromic photoPUSH layer bonded to a PUSH adhesive layer, used for environmental UV light monitoring demonstrated by a color change on a window. d) PUSH-based UV-sensor sticker for enclosure light monitoring in packaging applications.

stability and integration of all the PUSH composite elements (good dispersion and protection of the PMA, as well as good interlayer bonding strength), the sensing device is waterproof, and no loss in performance or function is observed after exposure to water before, during, and after sensing. In addition to skin, the UV detection patch can also be mounted on textiles. A top UV-sensing layer and a PUSH adhesive layer were successfully mounted on cotton textiles by attaching the PUSH layer to cotton fabric and heating at 80 °C, allowing the penetration of softened PUSH into the cotton fibers (Figure S14, Supporting Information). Similar to skin-mounted sensors, the color of the UV detector on cotton fabric turned to dark blue upon UV irradiation (Figure 5c), with the color change progressively monitored thanks to the reference bands.

We also fabricated an all-PUSH wearable wristband with integrated UV detection patches as depicted in Figure 5d. The wristband was fabricated from PUSH films, the reference bands from pre-exposed saturated photoPUSH films, and the detection patch from responsive photoPUSH, using the same

architecture and designs as the previous devices. The shade of blue color of the UV detector increased with increasing UV irradiation, progressively matching the colorimetric reference levels (Figure 5e(i,ii)). By comparing the wristband on a well-lit white background to a realistic application scenario (worn on the wrist, skin-mounted, or textile-mounted), the shades of blue colors are affected by the background. However, the color change due to background is consistent in all photoPUSH materials including the saturated reference bands, and therefore the evolution of the sensor can still be tracked without problems. If the background effect wants to be permanently removed, the versatile design of the device allows for additional components, and for example, a white (or other colors) layer can be integrated as a bottom background layer. Furthermore, due to the fact that the wristband is built from all-PUSH materials, it is stretchable and can be healed from extreme mechanical damage that would otherwise terminate the device function, including scratches, severe large deformation, tears, and cuts. As shown in Figure 5e(iii) and Figure S15 (Supporting
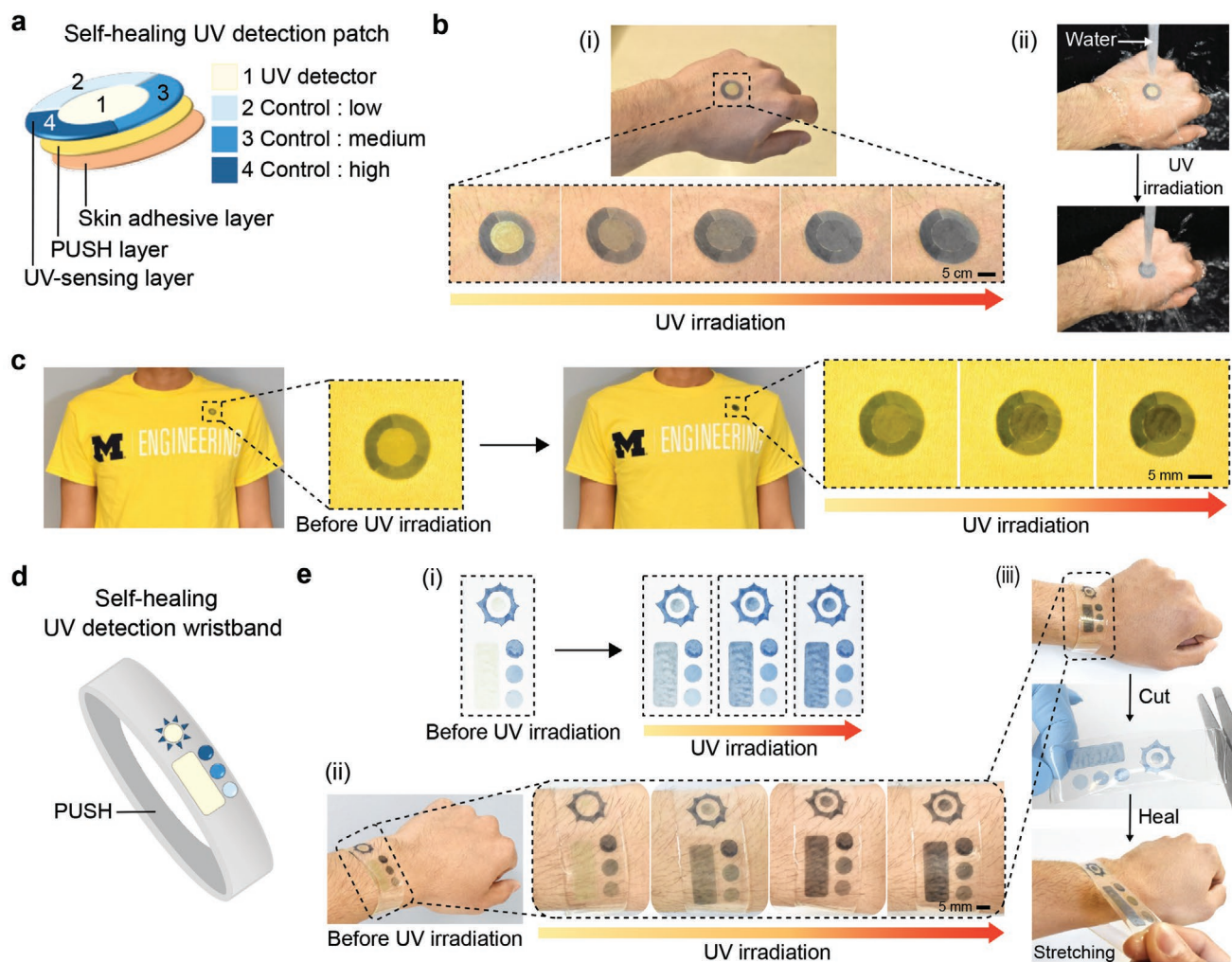
Figure 5. PUSH-based UV-monitoring wearables. a) PUSH-based UV detection patch including a photoPUSH sensing layer 1) and three saturated controls for colorimetric ref. [2–4]. b) Skin-mounted UV detection patch i) with color change upon UV irradiation ii) while being waterproof. c) Textile-mounted PUSH-based UV detector with color change upon UV irradiation. d) PhotoPUSH-based UV detection wristband containing UV detector and reference bands on a PUSH wristband. e) The UV detection wristband changes color upon UV irradiation i) on white background and ii) on human skin. iii) The self-healing UV detection wristband was cut into two pieces and subsequently healed, showing no loss of function and no visible damage upon stretching.

Information), the self-healing UV detection wristband was cut and consequently healed at 70 °C, enabling repair of the wristband and recovery of stretchability without loss of sensing function (however, in practical applications, we anticipate that the sensor would withstand minor damages such as scratches, delamination, or small cracks instead of deliberate extreme cuts, and therefore healing at lower temperatures would be appropriate). In addition, PUSH polymers provide waterproof protection of the PMA dopants, therefore enabling healing and sensing in wet environments (which is not possible with many sensor substrates that rely on electronics and on water-sensitive substrates) (Figure S15, Supporting Information). Due to the versatility of PUSH polymers as a multifunctional platform for photochromic devices, this approach could be extended to other photochromic active molecules for sensing (such as spiropyran, Figure S16, Supporting Information). The wearable sensing

devices demonstrated here (skin-mounted, textile-mounted, and wristband) have been designed and fabricated aiming for skin type I and for a MED of 200 kJ m^{-2} as described previously. However, these devices can easily be extended to other skin types by integrating UV filters to adjust the UV absorbance and detection threshold (therefore tuning the MED to match specific skin types). This will lead to wearable sensors that can be worn on the skin, on clothes, or as accessories, that can monitor the UV exposure in real-time and notify the user with a visual color cue when it reaches dangerous dose levels (MED). Because of the flexibility, stretchability, healing properties, and durability of PUSH polymers, these wearable materials and devices present excellent opportunities for sensing in challenging environments where UV exposure is overabundant and historically presents skin damage risks (Tables S1–S3, Supporting Information).

3. Conclusions

Self-healing photochromic composite elastomers (photoPUSH) are developed here by incorporating phosphomolybdic acid (PMA) into a dynamic polyurethane polymer network with reversible disulfide bonds (PUSH). The photoPUSH polymers displayed a color transformation from colorless to blue upon UV irradiation via photochromic reactions between the PMA molecules and electron donor groups in polyurethane structure of the elastomeric matrix. PhotoPUSH elastomers displayed excellent durability and no loss of performance under large strain deformations, in underwater environments (waterproof), and under extreme mechanical stress and severe damage. These properties arise from the multifunctional, dynamic polyurethane network, which simultaneously provides: i) electron donor functional groups to enable the photochromic mechanism, ii) excellent elastomeric properties (large deformations), durability, and protection of the photochromic dopants, iii) high-efficiency healing to recover the structural integrity of the materials and the device function, iv) adhesive properties, and v) strong interfacial bonding to enable the fabrication of architected devices and their attachment to surfaces. Taking advantage of these unique properties, we developed several soft, portable UV-sensing devices for applications in environmental monitoring, packaging, and wearables (including skin-mounted, textile-mounted, and wristband devices). These sensors change their color with UV irradiation and provide a visual cue to alert the user when a dose threshold has been reached. Due to the healing properties of the PUSH matrix, the fabrication approaches are very versatile and allow for the incorporation of multimaterial complex designs. For example, we have integrated multimaterial UV-filtering in the sensors to adapt their sensing range and their alert saturation threshold to the hazardous UV doses (MED) of different skin types, thus demonstrating the tunability of the sensors through materials design.

4. Experimental Section

Materials and Methods: Polytetrahydrofuran (PTHF, $M_n \approx 1000$ g mol^{-1}) was dried at 120 °C under vacuum for 2 h before use. 2-hydroxyethyl disulfide (HEDS, ≥ 85.0%), dibutyltin dilaurate (DBTDL, 95%), 4,4′-methylenebis(cyclohexyl isocyanate) (HMDI, 90.0%), 1,6-hexanediol (HDO, 99%) tetrahydrofuran (THF, ≥ 99.9%), N,N-dimethylacetamide (DMAc, ≥ 99.0%), phosphomolybdic acid hydrate (PMA), 2-propanol (IPA, ≥ 99.5%) were purchased from Sigma Aldrich and were used as received. 1,3,3-trimethylindolino-6′-nitrobenzopyrylospiran (SP, > 98.0%) was purchased from TCI Chemicals. Gel permeation chromatography (GPC, Shimadzu) was performed to estimate the apparent molecular weight of polymers with a refractive index detector and three columns arranged in series (3 Phenomenex Phenogel™ 10 μm Linear (2), LC Column 300 × 7.8 mm). Polymer solutions in THF were filtered through a 0.45 μm pore size PTFE membrane filter and measured at 40 °C with a flow rate of 1 mL min^{-1}. The system was calibrated with linear polystyrene standards. Fourier transform infrared spectroscopy (FTIR) spectra were recorded using an FTIR spectrometer (Nicolet iS20, Thermo Fisher Scientific) on Attenuated total reflectance (ATR) mode with a wavenumber range of 400–4000 cm^{-1} by 32 scans at a resolution of 4 cm^{-1}. Transmittance spectra were recorded using a UV–vis spectrometer equipped with a 60 mm collection integrating sphere (Lambda 750S, PerkinElmer).

Synthesis of Polyurethane Elastomers: PTHF (20.1 g, 20.1 mmol) was melted at 70 °C in a 500 mL round bottom flask connected to a digital overhead stirrer (RealTorqueDigital™, Fisherbrand) with a polytetrafluoroethylene-coated propeller. HMDI (15.3 mL, 62.8 mmol) was then added into the flask and stirred to give a well-mixed mixture, followed by addition of DBTDL (38 μL, 0.06 mmol). After 2 h, a viscous prepolymer solution was obtained and diluted with DMAc (80 mL). HEDS (5.1 mL, 41.7 mmol) was then charged into the solution and the reaction was allowed to proceed at 70 °C for another 16 h to obtain a self-healing polyurethane (PUSH). The solution of PUSH after reaction was diluted with DMAc (90 mL).

A polyurethane without self-healing ability (PUHD) was prepared following the same aforementioned procedure with PTHF (20.3 g, 20.3 mmol), HDMI (15.4 mL, 63.2 mmol), HDO (5.0 g, 42.7 mmol), and DMAc (100 mL) during 12 h of reaction and that DMAc (50 mL) and THF (20 mL) were used for diluting the polymer solution after reaction. The apparent weight-average molecular weight (M_w), the apparent number-average molecular weight (M_n), and the molecular weight distribution (MWD) of PUSH were 77 800 g mol^{-1}, 38 000 g mol^{-1}, and 2.05, respectively. The M_w, M_n, and MWD of PUHD were 153 800 g mol^{-1}, 81 500 g mol^{-1}, and 1.89, respectively. The diluted polymer solutions were dried at 60 °C in a vacuum oven for 5 d to obtain polymer films for further experiments.

Evaluation of Photochromic Properties of PMA on Different Substrates: Solutions of PMA in IPA (2 μL) with different concentrations (1.0, 2.5, and 5.0 mM) were dropped on different substrates (PUSH, PUHD, borosilicate glass, polyethylene terephthalate or PET, polystyrene or PS, Ecoflex, and Sylgard 184 polydimethylsiloxane or PDMS) using a 10-μL pipette tip. It was noted that a drop of the PMA solution on borosilicate glass, PET, PS, and PDMS was confined in a circular PDMS cavity (diameter ≈3 mm) to restrict spreading of the solution. The PMA solutions on substrates were dried at 25 °C for 24 h, followed by heating at 70 °C for 24 h and subjecting to UVA exposure at different times (180, 300, 600, and 900 s).

UV–vis Spectrophotometry Measurements of Self-Healing Photochromic Films: PUSH polymer was dissolved in a solution of PMA in DMAc with a concentration of 0.05, 0.1, 0.5, 0.8, 1.0, 2.5, 5.0, 10.0, and 15.0 mM, respectively at 25 °C for 20 h to prepare a solution of PMA/PUSH with a concentration of 0.08 g mL^{-1}. A solution of PUSH in pure DMAc (0.08 g mL^{-1}) was used as a control sample. The obtained solutions of PMA/PUSH in DMAc (250 μL) were cast on glass substrates (2.5 × 2.5 × 1.0 mm), followed by drying in the dark at 60 °C in a vacuum oven for 5 d to yield photoPUSH films (thickness = 0.02 mm) with 0.1, 0.2, 1.1, 1.8, 2.3, 5.7, 11.4, 22.8, and 34.2 wt.% PMA, respectively. UV irradiation on the specimens was performed in a UV light chamber (Fisherbrand) using 8-watt fluorescent tubes (USHIO America) with λ_{max} at 368, 306, and 265 nm for UVA, UVB, and UVC lights, respectively. The specimens were irradiated with an average light intensity of 37 ± 2, 54 ± 3, and 56 ± W m^{-2} for UVA, UVB, and UVC, respectively, which were monitored using an optical power meter (PM100A, ThorLabs) with a power sensor (S120VS, ThorLabs, aperture diameter = 9.50 mm). The dose of UV light is a quantity of UV light intensity multiplied by exposure time. For the evaluation of sensitivity to UVA, B, and C, the photoPUSH films (5.7 wt.% PMA) on glass substrate were subjected to UVA, B, and C light exposure with increasing UV doses from 0 to 400 kJ m^{-2}. For evaluation of photoPUSH with UV filters, the photoPUSH films were covered by UV filters (PET thin films) with different thicknesses (200, 400, 500, 600, and 800 μm), followed by exposure to UVA. UV–vis absorbances of the photoPUSH films were measured in triplicates using a microplate reader (Synergy HT, BioTek) at a wavelength range of 300–900 nm with increasing UVA exposure time from 0–180 min. To study the effect of temperature on photochromism, the photoPUSH films (5.7 wt.% PMA, thickness = 0.02 mm) were irradiated with an average UVA light intensity of 25 ± 1 W m^{-2} using a 365 nm UV lamp (5 watts, DARKBEAM) at different temperatures of 0 °C (Peltier cooling plate), 25 °C, and 70 °C (hot plate) for 150 min.

Reversible Color Transition of Photopush Composites: A photoPUSH composite (11.4 wt.% PMA) with blue color was immersed in an

**ADVANCED
SCIENCE NEWS**

www.advancedsciencenews.com

**ADVANCED
FUNCTIONAL
MATERIALS**

www.afm-journal.de

oxidizing solution (15 vol.% H_2O_2, 30 vol.% IPA, and 55 vol.% H_2O) at 25 °C for 16 h, and dried at 60 °C under vacuum for 2 d.

Durability and Mechanical Properties of Self-Healing Photochromic Elastomer: A solution of PMA in IPA (2 μL, 10.0 mM) was dropped on two different PUSH films (thickness = 0.24 mm), and then dried at 25 °C for 24 h to obtain a deposition of PMA on the PUSH films. An encapsulation of PMA in PUSH was prepared by covering another PUSH film over the deposited PMA, followed by heating at 70 °C in an oven for 24 h. A photoPUSH sample was prepared by attaching a circular photoPUSH with 5.7 wt.% PMA (diameter ≈3 mm) to a PUSH film, and then heating at 70 °C in an oven for 24 h. All samples were stretched with an elongation of ≈95% using a stretching device. Microscopy images were recorded using a digital microscope Dino-Lite AM73915MZTL (R10A) with an imaging software (Dinocapture 2.0). Samples for tensile test were prepared by casting a solution of PMA/PUSH (23 mL, 0.08 g mL^{-1}, 2.5 mM PMA in DMAc) on a glass petri dish (90 mm diameter), followed by drying in the dark at 60 °C in a vacuum oven for 5 d. PUSH and PUDH films were prepared by the same procedures for photoPUSH and used as control samples. The obtained polymer films were cut as dog-bone-shaped specimens with an overall length of 30 mm, a gauge length of 10 mm, and a width of 5 mm. The healed samples for photoPUSH and pure PUSH were prepared by cutting the pristine films in half using a cutter blade, then the two pieces were put together again and healed at 70 °C in an oven for 24 h. Mechanical tensile tests were performed in triplicates using a texture analyzer (TA.XT Plus, Stable Micro Systems) with a strain rate of 60 mm min^{-1} at 25 °C. The shear creeps measurements were performed using a Discovery HR30 rheometer (TA Instruments) with upper parallel plate and UV curing accessories, which were equipped with an Omnicure series1500 light source with a 320–390 nm UV light filter. A constant creep stress of 0.1 MPa was applied to PUSH films (Thickness ≈0.3 mm) for 900 s at 25 °C.

Adhesion Test of a Self-Healing Polymer to Substrates: The experiments were performed using the Discovery HR30 rheometer (TA Instruments) with parallel plates at 25 °C. A circular PUSH film (diameter = 10 mm, thickness = 0.03 mm) and sample substrates (PS, glass, polyethylene (PE), PET, stainless steel (SS), PUSH, paper, PDMS, sandpaper (1000 SiC grit), and cotton fabric) adhered to the top plate and the bottom plate, respectively using a double-sided adhesive tape. The adhesion tests were performed with 3 steps (1 cycle) as illustrated in Figure 4a. The PUSH film was moving down with a velocity of 10 μm s^{-1} to make a contact with the sample substrates until a compressive preload force of 2 N was reached (loading step). After a contact time of 10 s (contact step), the PUSH film was retracted from the sample substrates with a velocity of 10 μm s^{-1} (unloading step). The pull-off stress was the ratio of a maximum force before detachment to the contact area between the PUSH film and the sample substrates. The adhesion measurements were repeated in triplicates.

Fabrication and Demonstration of Self-Healing UV Sensor Stickers, UV Detection Patches, and UV Detection Wristbands: Pristine photoPUSH with 5.7 wt.% PMA (thickness ≈0.05 mm) were used as a UV sensor by cutting into sun-like and exclamation mark-like shapes using a cutter blade, which was consequently adhered to PUSH films (thickness ≈0.3 mm) and healed at 70 °C in an oven for 5 h to obtain self-healing UV sensor stickers (Figure 4d,e). The UV sensor stickers with sun-like and exclamation mark-like shapes were attached to a glass window and a cardboard box, respectively, which then were exposed to natural sunlight.

For UV detection patches and wristbands, photoPUSH with 1.1, 1.8, and 5.7 wt.% PMA (thickness = 0.05 mm) after being exposed to UVA light for 40 min were used as low, medium, and high reference colors of photoPUSH, respectively. A pristine photoPUSH with 5.7 wt.% PMA (thickness ≈0.05 mm) was used as a UV detector. The reference photoPUSH was cut into a third of donut-like shapes while the UV detector was prepared as a circular film. The prepared photoPUSH films were assembled by placing the circular UV detector at the center among the reference photoPUSH, followed by attaching to a PUSH film and healing at 70 °C in an oven for 5 h to obtain UV detection patches (Figure 5a). The UV detection patch was attached to skin using a double-sided skin adhesive tape (MaskTite, USA). For attaching

to cotton fabric, the UV detection patch was adhered to the fabric with a compression by being covered between glass substrates and compressed using binder clips (length = 32 mm), followed by heating at 80 °C in an oven for 24 h.

A self-healing wristband was prepared by entwining a rectangular PUSH polymer sheet (length = 16.5 cm, width = 2.5 mm, and thickness = 0.60 mm) around a glass cylinder, followed by healing at 70 °C in an oven for 24 h. The reference photoPUSH (diameter = 6 mm), a rectangular UV detector (2.2 mm × 9 mm), and a circular UV detector (diameter = 5 mm) inside with an eight-angled star-like control photochromic film were attached to the wristband as the design shown in Figure 5d, followed by healing at 70 °C in an oven for 5 h. The human participant to showcase the sensors gave explicit consent to the sensor demonstrations, which did not require IRB approval (HUM00225345).

Preparation of Self-Healing Photochromic SP/PUSH Composites: A solution of SP/PUSH with concentration of 0.08 g mL^{-1} was prepared by dissolving PUSH polymer in a solution of SP in DMAc (1 mM) at 25 °C. The polymer solution (450 μL) was cast on a glass substrate (2.5 × 2.5 × 1.0 mm), followed by drying in the dark at 60 °C in a vacuum oven for 3 d to yield a self-healing photochromic composite film with 0.4 wt.% SP. The SP/PUSH composite film was irradiated with UVA light (365 nm, 25 W m^{-2}) for 3 min to activate the color change. The reversibility of photochromism for SP/PUSH composite film is obtained upon heating at 60 °C in an oven for 3 min.

Supporting Information

Supporting Information is available from the Wiley Online Library or from the author.

Conflict of Interest

The authors declare no conflict of interest.

Data Availability Statement

The data that support the findings of this study are available in the supplementary material of this article.

**ADVANCED
SCIENCE NEWS**

www.advancedsciencenews.com

**ADVANCED
FUNCTIONAL
MATERIALS**

www.afm-journal.de

[1] J. Köhrle, M. Rauner, S. A. Lanham-New, *Endocr. Connect.* **2022**, *11*, 210609.

[2] Z. Xie, T. Fan, J. An, W. Choi, Y. Duo, Y. Ge, B. Zhang, G. Nie, N. Xie, T. Zheng, Y. Chen, H. Zhang, J. S. Kim, *Chem. Soc. Rev.* **2020**, *49*, 8065.

[3] D. S. Richardson, J. W. Lichtman, *Cell* **2015**, *162*, 246.

[4] M. Raeiszadeh, B. Adeli, *ACS Photonics* **2020**, *7*, 2941.

[5] United States Environmental Protection Agency, Health Effects of UV Radiation, https://www.epa.gov/sunsafety/health-effects-uv-radiation, (accessed: June, 2010).

[6] S. R. Pinnell, *J. Am. Acad. Dermatol.* **2003**, *48*, 1.

[7] E. R. Gonzaga, *Am. J. Clin. Dermatol.* **2009**, *10*, 19.

[8] D. McDaniel, P. Farris, G. Valacchi, *J. Cosmet. Dermatol.* **2018**, *17*, 124.

[9] B. K. Armstrong, A. Kricker, *J. Photochem. Photobiol. B, Biol.* **2001**, *63*, 8.

[10] M. R. Wehner, M. M. Chren, D. Nameth, A. Choudhry, M. Gaskins, K. T. Nead, W. J. Boscardin, E. Linos, *JAMA Dermatol.* **2014**, *150*, 390.

[11] H. R. Waters, A. Adamson, *J. Cancer Policy* **2018**, *17*, 45.

[12] Y. Shi, R. Pielak, G. Balooch, WO2017120176A1, **2017**.

[13] P. Wei, R. Pielak, Y. Shi, E. Messager, G. Balooch, US20190204146A1, **2018**.

[14] E. Dumont, S. Banerjee, M. Contreras, US20160364131A1, **2016**.

[15] W. Zou, M. Sastry, J. J. Gooding, R. Ramanathan, V. Bansal, *Adv. Mater. Technol.* **2020**, *5*, 1901036.

[16] X. Huang, A. N. Chalmers, *Ann. Biomed. Eng.* **2021**, *49*, 964.

[17] S. Cai, X. Xu, W. Yang, J. Chen, X. Fang, *Adv. Mater.* **2019**, *31*, 1808138.

[18] L. Jia, W. Zheng, F. Huang, *PhotoniX* **2020**, *1*, 22.

[19] W. Zheng, L. Jia, F. Huang, *iScience* **2020**, *23*, 101145.

[20] M. Razeghi, A. Rogalski, *J. Appl. Phys.* **1996**, *79*, 7433.

[21] F. Teng, K. Hu, W. Ouyang, X. Fang, *Adv. Mater.* **2018**, *30*, 1706262.

[22] W. Ouyang, F. Teng, J.-H. He, X. Fang, *Adv. Funct. Mater.* **2019**, *29*, 1807672.

[23] Y. Zou, Y. Zhang, Y. Hu, H. Gu, *Sensors* **2018**, *18*, 2072.

[24] A. B. A. Kayani, S. Kuriakose, M. Monshipouri, F. A. Khalid, S. Walia, S. Sriram, M. Bhaskaran, *Small* **2021**, *17*, 2100621.

[25] R. Pardo, M. Zayat, D. Levy, *Chem. Soc. Rev.* **2011**, *40*, 672.

[26] D. J. Wilson, F. J. Martín-Martínez, L. F. Deravi, *ACS Sens.* **2022**, *7*, 523.

[27] J. Zhang, Q. Zou, H. Tian, *Adv. Mater.* **2013**, *25*, 378.

[28] Y. Zheng, W. Panatdasirisuk, J. Liu, A. Tong, Y. Xiang, S. Yang, *Adv. Mater. Technol.* **2020**, *5*, 2000564.

[29] W. Jeong, M. I. Khazi, D.-H. Park, Y.-S. Jung, J.-M. Kim, *Adv. Funct. Mater.* **2016**, *26*, 5230.

[30] M. E. Lee, A. M. Armani, *ACS Sens.* **2016**, *1*, 1251.

[31] K. E. Lee, J. U. Lee, D. G. Seong, M.-K. Um, W. Lee, *J. Phys. Chem. C* **2016**, *120*, 23172.

[32] X. Dong, Y. Wei, J. Gao, X. Liu, L. Zhang, Y. Tong, Y. Lu, *J. Photochem. Photobiol. A* **2022**, *425*, 113716.

[33] B. Bao, J. Fan, Z. Wang, Y. Wang, W. Wang, X. Qin, D. Yu, *Compos. B. Eng.* **2020**, *202*, 108464.

[34] R. Wang, X. Lu, L. Hao, W. Jiao, W. Liu, J. Zhang, F. Yuan, F. Yang, *J. Mater. Chem. C* **2017**, *5*, 427.

[35] L. M. F. Tandy, J. J. P. Bueno, Y. M. Vong, I. Z. Torres, L. L. Rojas, C. J. R. Torres, H. M. Gutiérrez, M. L. M. López, *J. Sol-Gel Sci. Technol.* **2017**, *82*, 51.

[36] W. Zou, A. González, D. Jampaiah, R. Ramanathan, M. Taha, S. Walia, S. Sriram, M. Bhaskaran, J. M. Dominguez-Vera, V. Bansal, *Nat. Commun.* **2018**, *9*, 3743.

[37] J. Fan, B. Bao, Z. Wang, H. Li, Y. Wang, Y. Chen, W. Wang, D. Yu, *Chem. Eng. J.* **2021**, *404*, 126488.

[38] L. Li, Y.-C. Zou, Y. Hua, X.-N. Li, Z.-H. Wang, H. Zhang, *Dalton Trans.* **2020**, *49*, 89.

[39] S. Liu, H. Möhwald, D. Volkmer, D. G. Kurth, *Langmuir* **2006**, *22*, 1949.

[40] T. He, J. Yao, *Prog. Mater. Sci.* **2006**, *51*, 810.

[41] S. Cai, C. Zuo, J. Zhang, H. Liu, X. Fang, *Adv. Funct. Mater.* **2021**, *31*, 2100026.

[42] C. Lu, Y. Sun, J. Liu, X. Wang, S.-L. Liu, W. Feng, *J. Appl. Polym. Sci.* **2015**, *132*.

[43] G. Zhang, W. Yang, J. Yao, *Adv. Funct. Mater.* **2005**, *15*, 1255.

[44] J. Chen, L.-l. Dong, W. Feng, S.-L. Liu, J. Liu, F.-L. Yang, *J. Mol. Struct.* **2013**, *1049*, 414.

[45] J. Chen, L. Mei Ai, W. Feng, D. Q. Xiong, Y. Liu, W. M. Cai, *Mater. Lett.* **2007**, *61*, 5247.

[46] Y. J. Tan, G. J. Susanto, H. P. Anwar Ali, B. C. K. Tee, *Adv. Mater.* **2021**, *33*, 2002800.

[47] T. Yimyai, T. Phakkeeree, D. Crespy, *Adv. Sci.* **2020**, *7*, 1903785.

[48] J. Kang, J. B. H. Tok, Z. Bao, *Nat. Electron.* **2019**, *2*, 144.

[49] B. C. Tee, C. Wang, R. Allen, Z. Bao, *Nat. Nanotechnol.* **2012**, *7*, 825.

[50] A. Pena-Francesch, H. Jung, M. C. Demirel, M. Sitti, *Nat. Mater.* **2020**, *19*, 1230.

[51] S. Terryn, J. Brancart, D. Lefeber, G. Van Assche, B. Vanderborght, *Sci. Robot.* **2017**, *2*, aan4268.

[52] T. Yimyai, A. Pena-Francesch, D. Crespy, *Macromol. Rapid Commun.* **2022**, *43*, 2200554.

[53] L.-M. Ai, W. Feng, J. Chen, Y. Liu, W.-m. Cai, *Mater. Chem. Phys.* **2008**, *109*, 131.

[54] E. Papaconstantinou, *Chem. Soc. Rev.* **1989**, *18*, 1.

[55] M. T. Pope, A. Müller, *Angew. Chem., Int. Ed.* **1991**, *30*, 34.

[56] Y. Sun, X. Wang, Y. Lu, L. Xuan, S. Xia, W. Feng, X. Han, *Chem. Res. Chin. Univ.* **2014**, *30*, 703.

[57] X.-y. Wang, Q. Dong, Q.-l. Meng, J.-Y. Yang, W. Feng, X.-k. Han, *Appl. Surf. Sci.* **2014**, *316*, 637.

[58] E. C. De Fabo, F. P. Noonan, T. Fears, G. Merlino, *Cancer Res.* **2004**, *64*, 6372.

[59] F. R. de Gruijl, in *Methods in Enzymology*, Vol. *319*, Academic Press, Cambridge **2000**.

[60] F. P. Noonan, M. R. Zaidi, A. Wolnicka-Glubisz, M. R. Anver, J. Bahn, A. Wielgus, J. Cadet, T. Douki, S. Mouret, M. A. Tucker, A. Popratiloff, G. Merlino, E. C. De Fabo, *Nat. Commun.* **2012**, *3*, 884.

[61] J. Moan, A. Dahlback, R. B. Setlow, *Photochem. Photobiol.* **1999**, *70*, 243.

[62] H. Sun, N. Gao, J. Ren, X. Qu, *Chem. Mater.* **2015**, *27*, 7573.

[63] K. H. Kaidbey, P. P. Agin, R. M. Sayre, A. M. Kligman, *J. Am. Acad. Dermatol.* **1979**, *1*, 249.

[64] T. B. Fitzpatrick, *Arch. Dermatol.* **1988**, *124*, 869.